PERGAMON

Atmospheric Environment 35 (2001) 4995–5005

ATMOSPHERIC ENVIRONMENT

www.elsevier.com/locate/atmosenv

Chemical speciation of individual atmospheric particles using low-Z electron probe X-ray microanalysis: characterizing "Asian Dust" deposited with rainwater in Seoul, Korea

Chul-Un Ro[a,b,*], Keun-Young Oh[a], HyeKyeong Kim[b], Youngsin Chun[c], János Osán[d], Johan de Hoog[e], René Van Grieken[e]

[a] *Department of Chemistry, Hallym University, ChunCheon, KangWonDo 200-702, South Korea*
[b] *Institute of Environment & Life Science, Hallym Academy of Sciences, Hallym University, ChunCheon, KangWonDo 200-702, South Korea*
[c] *Climate Prediction Division, Korea Meteorological Administration, 460-18 Shindaebang-dong, Tongjak-gu, Seoul 156-720, South Korea*
[d] *KFKI Atomic Energy Research Institute, P.O. Box 49, H-1525 Budapest, Hungary*
[e] *Department of Chemistry, University of Antwerp, Universiteitsplein 1, B-2610 Antwerp, Belgium*

Received 7 November 2000; received in revised form 14 May 2001; accepted 21 May 2001

Abstract

Chemical speciation of individual microparticles is of much interest in environmental atmospheric chemistry; e.g. the determination of the elemental concentrations in individual atmospheric aerosol particles is important to study the chemical behavior of atmospheric pollution. Recently, an EPMA technique using an X-ray detector equipped with an ultra-thin window, allowing EPMA to determine concentrations of low-Z elements, such as C, N, and O, in individual particles of micrometer size, has been developed. This technique, called low-Z electron probe X-ray microanalysis (low-Z EPMA), is applied to characterize the water-insoluble part of "Asian Dust", deposited by washout in the form of rainwater during an Asian Dust storm event and collected in Seoul, Korea. In this study, it was demonstrated that the single particle analysis using low-Z EPMA provided detailed information on various types of chemical species in the sample. In addition to aluminosilicates, silicon oxide, iron oxide, and calcium carbonate particles, which are expected to be present, carbonaceous particles are also observed in a significant fraction. This unexpected finding that particle sample originated from an arid area contains significant amount of carbonaceous particles is supported by the investigation of a "China Loess" sample. In addition, we also performed single particle analysis for a local soil sample, in order to check the possible influence from local sources on "Asian Dust". The characteristics of the local soil particle sample, e.g. the types of aluminosilicate particles and the abdundance of particles with deviating chemical species, are clearly different from "Asian Dust" and "China Loess" samples, whereas those two are similar, implying that the "Asian Dust" sample was not much influenced by local sources.

Keywords: Aerosols; Single particle analysis; Electron probe X-ray microanalysis; Asian Dust; Light element analysis

1. Introduction

Detailed knowledge on the chemical composition and the morphology of individual particles on a micrometer scale is becoming increasingly important. For example, since particles in the atmosphere serve as active reaction

*Corresponding author. Present address: Department of Chemistry, Hallym University, ChunCheon, Kang WonDo 200-702, South Korea Tel.: +82-33-240-1428; fax: +82-33-256-3421.

E-mail address: curo@sun.hallym.ac.kr (C.-U. Ro).

1352-2310/01/$ - see front matter
PII: S1352-2310(01)00287-4

sites for chemical reactions occurring in the atmosphere, the characterization of individual atmospheric particles can provide much useful information about the source, reactivity, transport, and removal of atmospheric chemical species. Since the atmospheric particles are chemically and morphologically heterogeneous, and the average composition obtained by the traditional bulk analyses does not describe well the characteristics of the different particles, micro-analytical methods have proven to be useful for studying atmospheric particles. Electron probe X-ray microanalysis (EPMA) is capable of simultaneously detecting the chemical composition and morphology of a microscopic volume, such as a single atmospheric particle (Jambers et al., 1995).

Recently, an EPMA technique using an energy-dispersive X-ray (EDX) detector equipped with an ultra-thin window, allowing EPMA to determine concentrations of low-Z elements, such as C, N, and O, in individual particles of micrometer size, has been developed. In our previous study, it was found that excitation interactions between electrons and the matrix atoms and the geometric and matrix effects of electron-induced X-ray signals for low-Z elements in individual atmospheric microparticles can be described by Monte Carlo simulation (Ro et al., 1999). By the application of a quantification method, which employs Monte Carlo simulation combined with successive approximations, it was also shown that at least semi-quantitative specification of the chemical compositions can be done (Szaloki et al., 2000; Osan et al., 2000). Furthermore, the chemical species, in addition to chemical composition, in individual urban particles can be determined by the application of the low-Z EPMA (Ro et al., 2000). The determination of low-Z elements in individual environmental particles allows to improve the applicability of the single particle analysis; many environmentally important atmospheric particles, e.g. sulfates, nitrates, ammonium and carbonaceous particles, contain low-Z elements.

Application of wavelength-dispersive X-ray (WDX) detection is another possibility for quantitative low-Z element analysis; recently, it was shown that semi-quantitative WDX analysis, down to oxygen, is feasible even for irregularly shaped particles down to 0.8 μm in equivalent diameter (Weinbruch et al., 1997). The WDX approach has some advantages over EDX, in terms of its better detection limit for low-Z elements, due to its better peak-to-background ratio, and its superior energy resolution, resulting in a lower probability of the overlapping between low-Z element K-lines and L-lines of transition metals. However, most critically, the much higher current needed for the measurements in WDX limits its potential just to the particles to the most stable under electron bombardment.

In almost every spring, usually from March to May, "Asian Dust", originating from the arid areas in Central China, is transported into Eastern China, Korea, Japan and even the Pacific Ocean over the Yellow Sea and, sometimes, industrialized regions in China. While the Asian Dust travels a long-range distance, it could react with diverse chemical species and/or provide a reaction site for chemicals in the gas phase. Therefore, Asian Dust can possibly carry other chemical species together with the original soil components. Hence, increasing attention has been devoted to the study of physico-chemical characteristic changes of Asian Dust particles during long-range transport. Analyses of Asian Dust particles collected in China and Japan have been carried out by some researchers (Zhang and Iwasaka, 1999; Fan et al., 1996; Okada et al., 1990). These studies show that Asian Dust usually consists of Al, Si, Mg, Ca, Ti, Fe, together with S and Cl (Zhang et al., 1993). However, few detailed analyses of Asian Dust particles collected in Korea have been performed. Besides, the research mainly focused on the elemental composition by bulk analyses (Lee et al., 1990, 1993).

In this study, the microanalyses of the chemical composition of the water-insoluble part of "Asian Dust" sample, deposited by washout in the form of rainwater during an Asian Dust storm event and collected in Seoul, Korea, was carried out, using the low-Z EPMA technique, and it was demonstrated that this single particle analysis provided detailed information on various types of chemical species in the sample. We also present the results of single particle analysis for a "China Loess" and a local soil sample, which are compared with the Asian Dust sample.

2. Experimental section

2.1. Samples

Chemical compounds, generally present in atmospheric aerosol particles such as $CaCO_3$, KNO_3, Al_2O_3, NaCl, $CaSO_4 \cdot 2H_2O$, and Fe_2O_3, were used to evaluate the concentration calculation method using iterative simulations. These particulate standard samples were prepared from *pro analysis* grade solid chemical compounds. The grains were ground to microscopic size using an agate mortar. To avoid the additional X-ray absorption and spectral overlap possibly caused by the conductive coating on the sample, Ag foils were used as a conductive substrate material for the collection of the standard particles. The particles were suspended in 0.01 M *n*-hexane and a volume of 10 μl of the suspension was dropped by micro-pipette onto the surface of the Ag foil and dried in air.

"Asian Dust" was collected in the backyard of the Korea Meteorological Administration (located in Dong-Jack-Gu, Seoul, Korea) in the form of rainwater on 6 April 1999. The sampled Asian Dust originated from the

arid area located at the upper part of the Yellow River (38–48°N, 100–115°E) on 4 April 1999, and had drifted toward the Korean peninsula. It had been deposited by washout in the form of rainwater and the rainfall had continued from 4.45 p.m. on 5 April to 0.50 a.m. on 6 April 1999. The amount of precipitation was 15 mm and an Asian Dust storm event was observed at 3.30 p.m. just before the rainfall, in Seoul, Korea, according to the daily record provided by the Korea Meteorological Administration. The rainwater was collected during the rainfall using a glass box ($50 \times 50 \times 20\,cm^3$).

China Loess particles collected in the loess layer (1.8–2.5 m from the surface) in Gansu Province of China and a local soil particle sample collected in the backyard of the Korea Meteorological Administration were analyzed. The China Loess material, called CJ-1 Certified Reference Materials, is the product of the environmental CRM project based on environmental co-operation between China and Japan.

Samples of Asian Dust particles were prepared by depositing an aliquot of rainwater on the Ag foil using a micro-pipette, followed by drying the wet particles in air. The CJ-1 and the local soil particles were ground to microscopic size using an agate mortar, suspended in distilled water, and deposited on the Ag foil in the same way as the Asian Dust particles. Five hundred particles for the Asian Dust sample and 300 particles both for the CJ-1 and soil particles were analyzed.

2.2. EPMA measurements

The measurements for the individual particles collected on the Ag foil were done using a JEOL Superprobe 733 electron microprobe equipped with Oxford Link SATW ultra-thin window EDX detector. For the analysis, an accelerating voltage of 10 kV and a 0.5 nA beam current were used. X-ray spectra were collected for 10 s on all particles. To minimize possible damage of the microparticles by the irradiating electron beam and to prevent vaporization of the volatile chemical species under vacuum, the temperature of the sample stage was maintained at around −193°C using liquid nitrogen. A more detailed discussion of the measurement conditions is given elsewhere (Ro et al., 1999). Measurements on individual particles were carried out automatically in point analysis mode. The localization of the particles was based on inverse backscattered electron contrast. Morphological parameters such as diameter and shape factor were calculated by an image processing routine. These estimated geometrical data were set as input parameters for the quantification procedure. The net X-ray intensities for the elements were obtained by nonlinear least squares fitting using the AXIL program (Vekemans et al., 1994).

2.3. Data analysis

The intensities of the characteristic X-rays for each element obtained from the X-ray spectra of the individual particles were used as input data to determine the elemental concentrations by utilizing Monte Carlo calculation. A number of well-developed and rigorously tested quantification procedures are available in EPMA [e.g. ZAF and $\phi(\rho z)$ methods], especially for the analysis of bulk samples. However, these procedures are limited for low-Z element analysis of individual atmospheric microparticles (in view of the small size and variable shape of the particles and the important matrix effect for low-Z elements); therefore a quantification method, which employs a Monte Carlo simulation in combination with successive approximations, was used in this work. It is based on a modified version of the single scattering CASINO Monte Carlo program (Drouin et al., 1997; Hovington et al., 1997), which was designed to assess, for low-energy beam interaction, the generated X-ray and electron signals. The modified version of the CASINO program allows the simulation of electron trajectories in spherical, hemispherical and hexahedral particles located on a flat substrate (Ro et al., 1999). The simulation procedure determines also the characteristic and continuum X-ray flux emitted from the substrate material and the influence of the substrate material on the energy distribution of the exciting electrons. The algorithm to iteratively determine the elemental concentrations from measured X-ray intensities was implemented using a MS Visual C++ compiler. A more detailed description of the algorithm for the successive approximations is given elsewhere (Szaloki et al., 2000) and the overall procedure for the quantitative analysis is summarized in Fig. 1.

3. Results and discussion

3.1. Evaluation of the concentration calculation procedure

The quantification method based on Monte Carlo simulation combined with successive approximations was evaluated by comparing the atomic concentrations obtained from EPMA measurements with their nominal values. At least 10 independent analyses were performed for each type of standard particles with their diameters varying between 0.5 and 5 μm. Table 1 shows the comparison of the nominal (C_n) and calculated (C_c) average concentrations for $CaCO_3$, KNO_3, Al_2O_3, NaCl, $CaSO_4 \cdot 2H_2O$, and Fe_2O_3. The standard deviations of the average calculated concentration (σ_c) depend on the fluctuations in the shape and size parameters of the particles. The relative differences in averages between the nominal and calculated concentra-

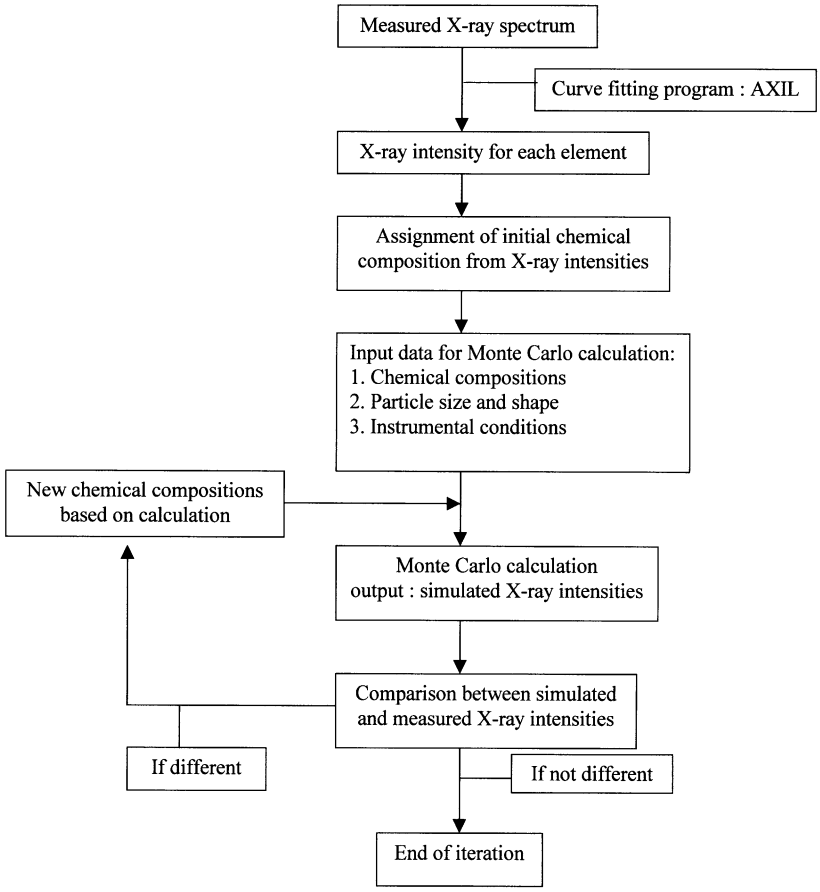

Fig. 1. Summary of the overall procedure for quantitative particle analysis based on the EPMA data.

tions are shown in the last column of the table. Even though diverse chemicals with different chemical and physical properties were used, these relative differences are within 12%, except for $CaCO_3$ and KNO_3, where the C and K contents are significantly different from their nominal concentrations. The Ag foil used as a collecting substrate shows an M_ζ X-ray peak ($E = 0.312$ keV) in the low energy region, overlapping with the C K_α X-ray peak ($E = 0.277$ keV). The Ag M_ζ peak for the pure Ag foil was fitted using the AXIL curve fitting program and the ratio of intensities between Ag L_α and M_ζ X-ray lines was obtained. In the calculation of the C content of particles, the apparent C K_α intensity, if any, was thus corrected for the influence of the Ag M_ζ line. Since the correction was done by applying the intensity ratio between Ag L_α and M_ζ X-ray lines for pure Ag foils, this first approximation will always overcorrect the influence of the Ag substrate on the intensity of the carbon X-ray peak; some X-rays from the Ag substrate sitting under particles will pass through the particles before being detected and the L X-rays are less absorbed by the particles than the M X-rays which have a lower energy. As shown in Table 1, the calculated C content of $CaCO_3$ particles is consistently lower than the nominal concentration due to this overcorrection. The energy of the K K_α X-ray is 3.314 keV and those of the Ag L_β X-ray lines are in the range of 3.150–3.350 keV; the K K_α X-ray line thus completely overlaps with the Ag L lines. The correction for the overlap of the Ag L_β X-rays on the K K_α was done by using the ratio between the intensities of the Ag L_α and L_β lines. In this case, the ratio value of the intensities obtained from pure Ag foils would hold because the energies of the Ag L_α and L_β X-rays are similar and thus the amount of the Ag L_α X-rays absorbed by particles would be similar to that of the L_β X-rays. However, if the size of the particle is small and the intensities of the Ag L X-rays are much stronger than those of the K K_α X-rays, the calculation of the intensity of the net K K_α X-rays is less accurate. In other words, the accuracy of the calculation is dependent on the particle size and that is why the standard deviation of the average calculated concentration (σ_c) is large for

Table 1
Comparison of nominal (C_n) and calculated (C_c) concentrations in atomic fraction for standard particles. The standard deviation of C_c is σ_c. The relative differences between calculated and nominal concentrations (in atomic fraction) are assigned as Δ in percentage

	C_n (in %)	C_c (in %)	σ_c	Δ (in %)
$CaCO_3$				
C	20.0	15.7	2.0	21.4
O	60.0	66.5	2.3	10.9
Ca	20.0	17.8	1.2	11.2
KNO_3				
N	20.0	22.9	3.3	14.5
O	60.0	52.7	8.6	12.2
K	20.0	24.4	11.0	22.1
Al_2O_3				
O	60.0	57.6	2.3	4.1
Al	40.0	42.1	2.3	5.2
NaCl				
Na	50.0	51.3	7.4	2.5
Cl	50.0	48.7	7.4	2.5
$CaSO_4 \cdot 2H_2O$				
O	75.0	72.5	2.4	3.4
S	12.5	14.0	1.4	12.0
Ca	12.5	13.5	1.3	8.3
Fe_2O_3				
O	60.0	62.6	2.8	4.3
Fe	40.0	37.5	2.8	6.4

K (see KNO_3 data in Table 1). Except for C and K, the procedure for elemental quantification is quite reliable. It was demonstrated elsewhere (Ro et al., 2000; Szaloki et al., 2000) that, when Al foil is used as the collecting substrate, the Monte Carlo calculation combined with the successive approximation provides at least semi-quantitative elemental concentrations, including for C and K.

3.2. Determination of chemical species in individual "*Asian Dust*" particles

The low-Z EPMA technique was applied to characterize the water-insoluble part of an Asian Dust sample collected in Seoul, Korea, on 6 April 1999. The analysis of the water-insoluble part of the Asian Dust sample is not expected to provide much useful information on the chemical modification of the Asian Dust, which may happen during its long-range transport, because chemical products from atmospheric reactions would be mostly water-soluble, such as sulfates and nitrates. With this limitation, our study mainly focused on the detailed characterization of soil-derived particles, which are water-insoluble, in the Asian Dust sample. However, it should be noticed that our work is the first demonstration that even chemical species in individual Asian Dust particles can clearly be identified.

Many distinctive particle types were identified, according to their chemical composition (see Table 2). Since this technique can determine the chemical species at least semi-quantitatively, some individual particles were identified as internal mixture particles, which are composed of two or more chemical species. However, it is somewhat difficult to clearly determine if particles are composed of only one chemical species or more, especially for aluminosilicates species. For geologists, it is well known that there exist many different types of aluminosilicate minerals; e.g., K-containing ones such as kaliophylite ($KAlSiO_4$), leucite ($KAlSi_2O_6$), and microcline ($KAlSi_3O_8$), Na-containing albite ($NaAlSi_3O_8$), analcite ($NaAlSi_2O_6 \cdot H_2O$), and natrolite ($Na_2Al_2Si_3O_{10} \cdot 2H_2O$), Mg-containing pyrope ($Mg_3Al_2Si_3O_{12}$), and serpentine ($Mg_3Si_2O_5(OH)_4$), and Ca-containing anorthite ($CaAl_2Si_2O_8$), chabazite ($Ca[Al_2Si_4O_{12}] \cdot 6H_2O$), clinozoisite ($Ca_2Al_3Si_3O_{12}(OH)$), gehlenite ($Ca_2Al_2SiO_7$), and grossularite ($Ca_3Al_2Si_3O_{12}$), etc. Our analysis showed, however, that soil-derived aluminosilicate particles are composed of mainly Al and Si oxides with either one or more minor elements, such as K, Na, Mg, Ca, S, Cl, Fe, and some heavy metals. Therefore, aluminosilicates are differently grouped according to the presence of minor elements, e.g., AlSi/K for aluminosilicate particles with minor K content. Detection limits of ED-EPMA for bulk sample are known to be 0.1–1.0% in weight due to its high background level. Since single particle analysis deals with microscopic volumes (pg range in mass), the detection limits may be worse, and thus some trace elements present may be missed. In this analysis, elements are judged to be present when their calculated concentrations are larger than 1%.

For the other types of particles, such as $CaCO_3$, SiO_2, and carbonaceous particles, it is somewhat easier to judge if some single particles are composed mainly of one of those species. However, even for very "pure" individual particles, it is common to also observe other minor chemical species. We defined, somewhat arbitrarily, a guideline; particles are classified as being composed of one chemical species when the species constituted at least 90% of the atomic concentration. As an illustration, three X-ray spectra of $CaCO_3$ particles are shown in Fig. 2. Certainly, the particle shown in Fig. 2(a) is composed of only, within detection limits, the $CaCO_3$ species and Fig. 2(c) is for a mixture particle of $CaCO_3$ and aluminosilicate minerals ($\sim$55% of $CaCO_3$ species in atomic fraction). The particle of Fig. 2(b) needs a decision for specification. It contains some minor aluminosilicate content. However, the

Table 2
Particle type and the numbers of particle found in the particle samples

Asian Dust			China Loess			Local soil		
	No. of particles	In %		No. of particles	In %		No. of particles	In %
AlSi[a]	24	4.8				AlSi	12	4.0
AlSi/Mg	61	12.2	AlSi/Mg	13	4.3	AlSi/K	49	16.3
AlSi/Mg/Fe	41	8.2	AlSi/Mg/Fe	12	4.0	AlSi/Na	4	1.3
AlSi/Mg/Na	8	1.6				AlSi/Fe	7	2.3
AlSi/Mg/Na/Fe	13	2.6				AlSi/K/Fe	27	9.0
AlSi's[b]/carb.	180	36.0	AlSi's/carb.	190	63.3	AlSi/K/Mg	13	4.3
AlSi's/SiO_2	10	2.0	AlSi's/SiO_2	3	1.0	AlSi/Mg/Fe	6	2.0
AlSi's/SiO_2/carb.	8	1.6				AlSi/K/Mg/Fe	7	2.3
AlSi's/$CaCO_3$	19	3.8	AlSi's/$CaCO_3$	16	5.3	AlSi's/carb.	88	29.3
AlSi's/$CaCO_3$/carb.	12	2.4	AlSi's/$CaCO_3$/carb.	6	2.0	AlSi's/SiO_2	9	3.0
Other AlSi's[c]	40	8.0	Other AlSi's[d]	13	4.3	Other AlSi's[e]	12	4.0
SiO_2	5	1.0	SiO_2	6	2.0	SiO_2	7	2.3
Carb.[f]	20	4.0	Carb.	23	7.7	Carb.	34	11.3
SiO_2/carb.	9	1.8	SiO_2/carb.	9	3.0	SiO_2/carb.	7	2.3
$CaCO_3$	6	1.2	Carb./Na	3	1.0	C/Na/S	3	1.0
$CaCO_3$/Mg	5	1.0				C/Al/P/Cl	4	1.3
Cl/C/O	6	1.2				C/N/O/S	3	1.0
Others[g]	17	3.4	Others[h]	1	0.3	Others[i]	1	0.3
NEIC[j]	16	3.2	NEIC	5	1.7	NEIC	7	2.3
Sum	500	100.0		300	100.0		300	100.0

[a] AlSi: aluminosilicate which contains almost exclusively Al, Si, and O as elements.
[b] AlSi's: aluminosilicates with minor elements such as Mg, K, etc.
[c] Other AlSi's types which are observed with less than 1.0% frequency (25 types: AlSi/K, AlSi/Na, AlSi/Cl, AlSi/Mg/K, AlSi/Mg/P, AlSi/Mg/Ca, AlSi/Mg/S, AlSi/Mg/Ca/Fe, AlSi/Mg/Cl/Ca, AlSi/Mg/P/Fe, AlSi/Mg/Na/Ca, AlSi/Mg/Cu/Fe, AlSi/Mg/K/Fe, AlSi/Mg/S/Ca, AlSi/Mg/S/Fe, AlSi/Mg/Ti/Fe, AlSi/Mg/Na/S, AlSi/Mg/Na/S/Cl, AlSi/Mg/Na/Cl/Fe, AlSi/Mg/Na/Mn/Fe, AlSi/Mg/Na/Cu/Fe, AlSi's/FeO_x, AlSi's/FeO_x/C, AlSi's/TiO_x, AlSi's/Ca/P/O).
[d] Other AlSi's types with less than 1.0% frequency (11 types: AlSi, AlSi/K, AlSi/Mg/Ca, AlSi/Mg/Ca/Fe, AlSi/Mg/K, AlSi/Mg/K/Fe, AlSi/Mg/Cl/Ca, AlSi/Na, AlSi/Na/Mg, AlSi/Na/Mg/Ca/Ti/Fe, AlSi's/TiO_x).
[e] Other AlSi's types with less than 1.0% frequency (10 types: AlSi/Mg, AlSi/Ti, AlSi/Na/Fe, AlSi/Ti/Fe, AlSi/K/Mn/Fe, AlSi/K/Ti/Fe, AlSi/K/Na/Fe, AlSi/K/Na/V/Fe, AlSi's/FeO_x, AlSi's/TiO_x).
[f] Carb.: carbonaceous species.
[g] Particle types with less than 1.0% frequency (6 types: $CaSO_4$, Ca/P/O, Cl/O, $CaCO_3$/Na, CuO_x/carb., SiO_2/Mg).
[h] Particle types with less than 1.0% frequency (1 type: $CaCO_3$).
[i] Particle types with less than 1.0% frequency (1 type: $CaCO_3$).
[j] NEIC: Not enough information for classification contained in X-ray data.

content of $CaCO_3$ species is larger than 90% in atomic fraction, and thus the particle is classified as a $CaCO_3$ particle. This approach, even though arbitrary, is necessary, because it is rare to observe particles composed of just one chemical species in 100% atomic fraction. Sometimes, there are cases where X-ray data are too ambiguous to clearly deduce information on chemical species and then just chemical elements observed are specified in the particle type name.

Table 2 shows the overall composition of water-insoluble Asian Dust particles characterized using the low-Z EPMA technique. The dominant chemical species are various types of aluminosilicates; some of them just contain aluminum, silicon and oxygen (24 particles; 4.8%), which is expressed as "AlSi" in Table 2. Most of aluminosilicates contain other elements, such as Na, Mg, Cl, K, P, Ca, Fe and some heavy metals. With different chemical elements present as minor species, 26 different types of aluminosilicate mineral particles are specified and the total number of these particles is 183 (37%). Several particle types, where aluminosilicates species exist with other chemical species such as $CaCO_3$, SiO_2, and carbonaceous species, are also observed; their total abundance is 235 among 500 particles measured (47%). The aluminosilicates species are the most frequently observed in this sample; their total abundance is 88% if all particles containing aluminosilicates species are counted in.

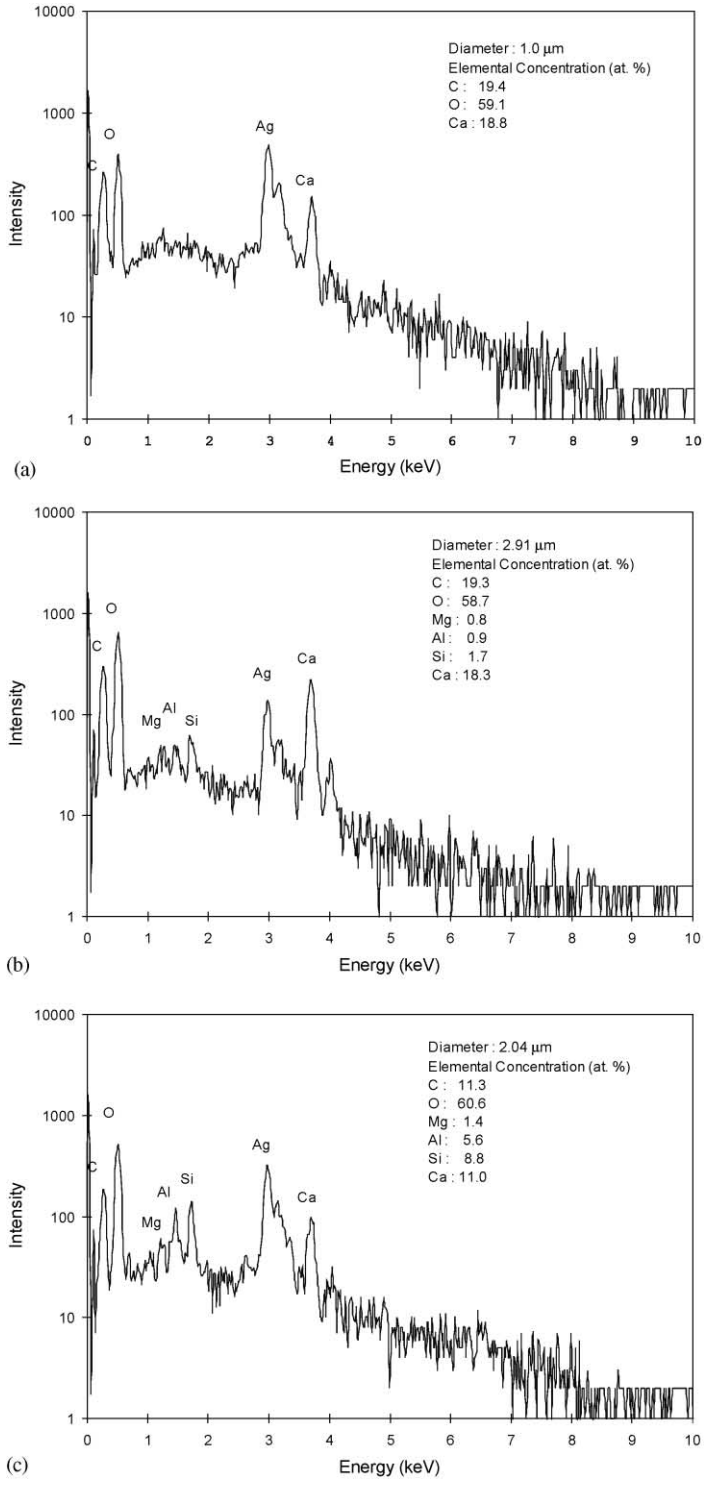

Fig. 2. X-ray spectra of $CaCO_3$ particles (a) of single species, (b) with minor aluminosilicate content, and (c) in mixture with aluminosilicate species.

Also, $CaCO_3$ and SiO_2 species are observed in significant fractions. Although the particles with single chemical species are much less frequently observed (1.0% for SiO_2 and 1.2% for $CaCO_3$ species), they mostly exist with other chemical species, such as aluminosilicates and carbonaceous species; 39 (7.8%) for $CaCO_3$ and 30 (6.0%) for SiO_2 species.

Carbonaceous particles are also significantly observed. This finding is not expected; the particles of the Asian Dust sample originated from an arid region in China and the carbonaceous species may not exist significantly. However, from the analysis of a China Loess sample, which is discussed later, it is confirmed that the carbonaceous species is indeed one of the essential ingredients of China Loess soil. Since the detection of hydrogen is not possible in EPMA, it is somewhat difficult to clearly specify the carbonaceous particles even though it was demonstrated that the carbonaceous particles can be identified as one of either elemental, organic, or biogenic particles using the low-Z EPMA technique (Ro et al., 2000). In this work, it was not attempted to specify the carbonaceous species in more detail because they are, we believe, mainly from humic substances. Carbonaceous particles are observed in various types, e.g. as a single species (20 particles; 4.0%), and mixtures with aluminosilicates (180; 36%), SiO_2 (17; 3.4%), and $CaCO_3$ (12; 2.4%). The total frequency to observe the carbonaceous species is 241 (48%), which suggests that the carbonaceous species should be considered as one of the important chemical species in Asian Dust particles.

The number distribution of the Asian Dust particles according to size is shown in Fig. 3. Since the mineral particles are irregularly shaped (see an illustrative secondary electron image in Fig. 4 (a)), the sizes of individual particles are calculated in equivalent diameter from the backscattered electron image (see Fig. 4(b)) using home-made software. Since the measurements were done only for particles larger than 0.5 μm size, this result does not provide information on particles smaller than that size. The number distribution for all particles shows that the most frequent size is in the range of 0.8–1.0 μm, with three additional shoulders at 1.3, 3.2, and 6.3 μm sizes. Mostly they have sizes in the range of 0.5–4.0 μm diameter. Also, two number distributions are shown in Fig. 3 for aluminosilicate particles of only one chemical species, and carbonaceous particles that are mostly existing as a mixture with aluminosilicates species. The number distribution for aluminosilicate particles shows a maximum at 0.6 μm and a peak value at 1.3 μm. In contrast, it is observed that there are two maxima at 0.8 and 1.3 μm and an additional peak at 6.3 μm, for carbonaceous particles. Also, the overall size of the carbonaceous particles is larger than that of aluminosilicates. This result implies that the carbonaceous species had existed heterogeneously with aluminosilicates species, and then some of the mixture particles were further broken down by some physical processes to produce smaller aluminosilicate particles. The peak at 6.3 μm in the overall distribution seems to be due to the carbonaceous particles and the peak at 3.2 μm is due to particles with other species.

3.3. Comparison of characteristics of "*Asian Dust*" with China Losse and local soil particle samples

Even though the Asian Dust particles were collected during an Asian Dust storm event, we were concerned

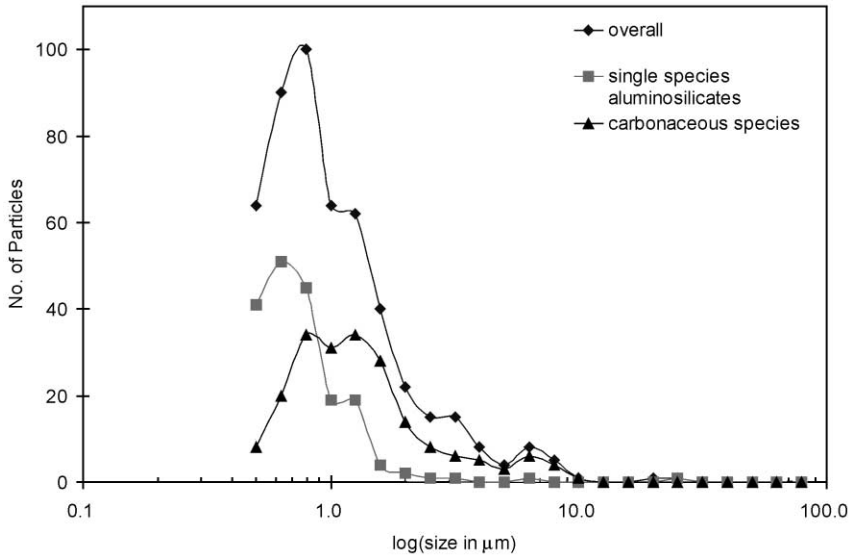

Fig. 3. Number distribution of Asian Dust particles according to their size.

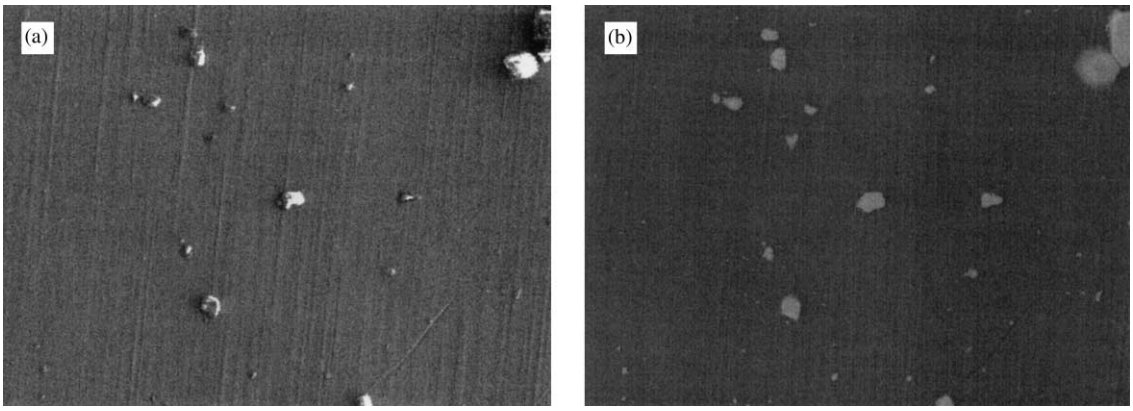

Fig. 4. Illustrative (a) secondary and (b) backscattered electron images for Asian Dust particles.

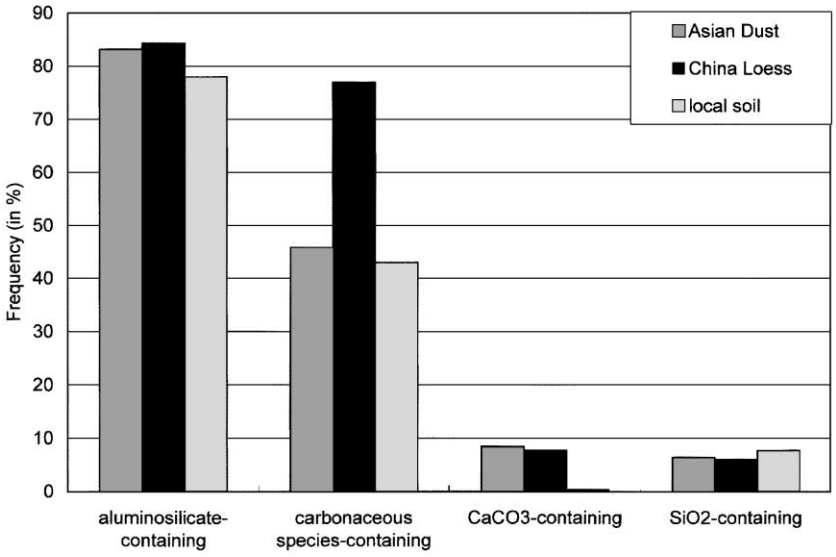

Fig. 5. Frequencies of four major chemical species observed in Asian Dust, China Loess, and local soil particle samples.

with the possibility of the influence from local sources, especially due to the observation of abundant carbonaceous particles. In order to address this question, 300 particles from both China Loess and local soil samples were analyzed and the overall composition of all these particles is also shown in Table 2.

For the China Loess sample, the carbonaceous particles are observed to be much more abundant than the Asian Dust sample; the fraction of carbonaceous particles with aluminosilicates species is 63% for the China Loess and 36% for the Asian Dust and that of carbonaceous particles is 7.7% vs. 4.0%. This result confirms that the China Loess soil indeed contains significant amount of carbonaceous species, most probably from humic substances. The reason why the China Loess sample has a higher carbonaceous content than the rain-collected Asian Dust may be explained as follows. The China Loess sample was ground using an agate mortar and thus this physical breaking-down process must be somewhat different from natural process which the Asian Dust particles experienced. We observed the difference between two size distributions of the Asian Dust and China Loess particles, where sizes of the China Loess particles are somewhat bigger (mostly in 0.8–5.0 μm range). As discussed earlier, the carbonaceous species in the Asian Dust sample seem to have existed heterogeneously with aluminosilicates species, and then some of the mixture particles were further broken down to produce smaller aluminosilicate particles. The China Loess particles were not as much microscopically broken down as the Asian Dust, and thus the chance to observe the carbonaceous species

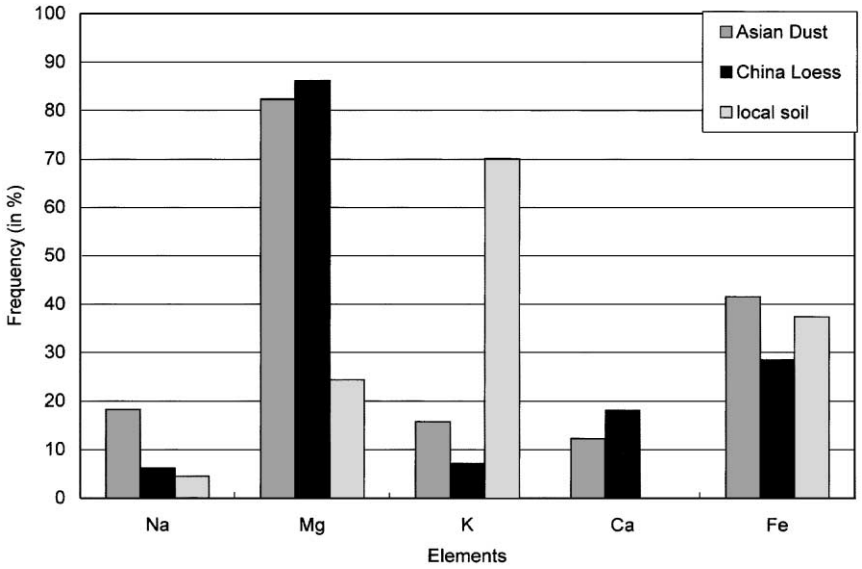

Fig. 6. Frequencies of major elements observed in aluminosilicate-containing particles of Asian Dust, China Loess, and local soil particle samples.

with the aluminosilicates species is higher in the China Loess sample, resulting in its higher frequency to encounter the particles containing carbonaceous species.

In Fig. 5, the observed frequencies of four major chemical species, e.g. aluminosilicates, carbonaceous, $CaCO_3$, and SiO_2 species, in three samples, are shown. The frequencies are calculated for particles which contain these species either as single species or mixtures. Particles containing aluminosilicates species are the most abundant, and carbonaceous species are the next. The abundance of SiO_2 containing particles is similar between the samples. However, it is quite different for $CaCO_3$ species; the local soil does not have the $CaCO_3$ species, but the Asian Dust and China Loess do have significantly.

Even though the abundance of particles containing aluminosilicates species is similar between the samples, there are some differences in chemical composition between particle samples originated from China (the Asian Dust and China Loess samples) and local soil sample. Fig. 6 shows the frequencies of the elements most frequently encountered in aluminosilicate-containing particles. In Asian Dust and China Loess samples, those aluminosilicate-containing particles also contain almost always Mg. In contrast, K is the most frequently encountered element in aluminosilicate-containing particles of the local soil sample. It implies that the Asian Dust and China Loess samples contain mostly Mg-enriched aluminosilicate minerals, whereas the local soil sample contains K-enriched minerals. Another difference in chemical composition of those aluminosilicate-containing particles is the absence of Ca element in the local soil sample. Na element is more encountered in the Asian Dust sample than the other two, implying the possible reaction between the Asian Dust and sea-salt particles while the Asian Dust particles crossed the Yellow Sea.

4. Conclusions

In this work, the water-insoluble part of Asian Dust, deposited by washout in the form of rainwater and collected in Seoul, Korea, during an Asian Dust storm event, is characterized using the low-Z EPMA. Detailed information on chemical composition and size distribution of the Asian Dust particle sample is provided by this single particle analysis technique. From the comparison study between the Asian Dust, China Loess, and local soil samples, it may be concluded that the Asian Dust particles were not much influenced by local sources because the characteristics of the Asian Dust sample are much more similar to those of China Loess sample. Particles with carbonaceous species are abundantly observed in the Asian Dust sample. By investigating size distributions of particles containing aluminosilicates and carbonaceous species, it seems that some of the particles containing aluminosilicates and carbonaceous species were broken up into individual particles of single chemical species. We are currently developing a methodology to characterize the heterogeneity of individual particles, which may be useful to study in more detail the physicochemical characteristic changes of Asian Dust particles during long-range transport.

Acknowledgements

This work was supported by Grant (HMP-99-M-09-0005) of 1999, Good Health R&D project, Ministry of Health Welfare, Republic of Korea. Also, the authors thank Prof. Kim Yoon-Shin in Han Yang University for making the CJ-1 materials available for our work.

References

Drouin, D., Hovington, P., Gauvin, R., 1997. CASINO: a new Monte Carlo code in C language for electron beam interactions—part II: tabulated values of the Mott cross section. Scanning 19, 20–28.

Fan, X.B., Okada, K., Nimura, N., Kai, K., Arao, K., Shi, G.Y., Qin, Y., Mitsuta, Y., 1996. Mineral particles collected in China and Japan during the same Asian Dust-storm event. Atmospheric Environment 30, 347–351.

Hovington, P., Drouin, D., Gauvin, R., 1997. CASINO: a new Monte Carlo code in C language for electron beam interaction—part I: description of the program. Scanning 19, 1–14.

Jambers, W., De Bock, L., Van Grieken, R., 1995. Recent advances in the analysis of individual environmental particles: a review. Analyst 120, 681–692.

Lee, M.H., Hwang, K.H., Kim, E.S., 1990. Dynamics of air pollutants during the Yellow Sand phenomena. Journal of Korean Air Pollution Research Association 6, 183–191.

Lee, M.H., Han, E.J., Shin, C.K., Han, J.S., Kim, S.K., 1993. Behavior of inorganic components in atmospheric aerosols during the Yellow Sand phenomena. Journal of Korean Air Pollution Research Association 9, 230–235.

Okada, K., Naruse, H., Tanaka, T., Nemoto, O., Iwasaka, Y., Wu, P.M., Ono, A., Duce, R.A., Uematsu, M., Merrill, J.T., 1990. X-ray spectrometry of individual Asian dust-storm particles over the Japanese islands and the North Pacific Ocean. Atmospheric Environment 24, 1369–1378.

Osan, J., Szaloki, I., Ro, C.-U., Van Grieken, R., 2000. Light element analysis of individual microparticles using thin-window EPMA. Mikrochimica Acta 132, 349–355.

Ro, C.-U., Osan, J., Van Grieken, R., 1999. Determination of low-Z elements in individual environmental particles using windowless EPMA. Analytical Chemistry 71, 1521–1528.

Ro, C.-U., Osan, J., Szaloki, I., Van Grieken, R., 2000. Determination of chemical species in individual aerosol particles using ultrathin-window EPMA. Environmental Science and Technology 34, 3023–3030.

Szaloki, I., Osan, J., Ro, C.-U., Van Grieken, R., 2000. Quantitative characterization of individual aerosol particles by thin-window electron probe microanalysis combined with iterative simulation. Spectrochimica Acta B55, 1017–1030.

Vekemans, B., Janssens, K., Vincze, L., Adams, F., Van Espen, P., 1994. Analysis of X-ray spectra by iterative least squares (AXIL): new developments. X-Ray Spectrometry 23, 278–285.

Weinbruch, S., Wentzel, M., Kluckner, M., Hoffman, P., Ortner, H.M., 1997. Characterization of individual atmospheric particles by element mapping in electron probe microanalysis. Mikrochimica Acta 125, 137–141.

Zhang, D., Iwasaka, Y., 1999. Nitrate and sulfate in individual Asian dust-storm particles in Beijing, China in spring of 1995 and 1996. Atmospheric Environment 33, 3213–3223.

Zhang, X., Arimoto, R., An, Z., Chen, T., Zhang, G., Zhu, G., Wang, X., 1993. Atmospheric trace elements over source regions for Chinese dust: concentrations, sources and atmospheric deposition on the Loess plateau. Atmospheric Environment 27A, 2051–2067.